Measurement of Methane Autoignition Delays in Carbon Dioxide Diluent at Supercritical Conditions

Miad Karimi[1], Bradley Ochs[1], Zefang Liu[1], Devesh Ranjan[1,2], Wenting Sun[1,2]
[1]School of Aerospace Engineering, Georgia Institute of Technology, Atlanta, GA 30332
[2]School of Mechanical Engineering, Georgia Institute of Technology, Atlanta, GA 30332
Georgia Institute of Technology
Atlanta, Georgia, USA

1 Introduction and background

The directly fired supercritical carbon dioxide (sCO_2) power cycle enables the dual benefit of high efficiency and nearly complete capture of CO_2. Different from conventional gas turbines, the operating conditions of the sCO_2 power cycle features high CO_2 concentration as diluent and extremely high pressures ranging from 100 bar to 300 bar, above the critical pressure of CO_2. Currently, there are no records on combustion properties at these conditions. This work reports the measurement of autoignition delays of $CH_4/O_2/CO_2$ mixtures at sCO_2 conditions for the first time and answers several open chemical kinetics questions at sCO_2 conditions: (a) Does chemically reactive CO_2 significantly alter ignition chemistry at high pressure conditions? (b) Are existing kinetic models derived mostly from data obtained at lower pressures capable of predicting autoignition delays at sCO_2 conditions?

In this work, autoignition delays of $CH_4/O_2/CO_2$ mixtures are measured above the critical point of CO_2 (at an average pressure of 100 bar and in the temperature range of 1274 to 1433 K) in a high-pressure shock tube with large inner diameter (15.24 cm). The large diameter is critical to this study as CO_2 diluent magnifies the non-ideal effect and increases the thickness of the boundary layer. High Mach number required for achieving the above conditions further increases shock attenuation mainly from wall viscous effects [11]. Therefore, a large diameter shock tube is required to avoid interaction between the boundary layer and the center region.

2 Experimental methods

A high pressure shock tube is used to measurement autoignition delays. The shock tube used in this study is fabricated out of 316 stainless steel with 15.24 cm inner diameter and a wall thickness of 5.08 cm. The total length of the shock tube is 20 m consisting of a 10 m long driver section (only 6 m used for this study) and a 10 m long driven section. The inner surface of the tube is electro polished with a 0.2 µm surface finish. The shock tube is equipped with six endwall plugs and eight circumferential ports (located 1.24 cm away

Correspondence to: W. Sun: wenting.sun@aerospace.gatech.edu; D. Ranjan: devesh.ranjan@me.gatech.edu

from the endwall) enabling pressure and optical measurements. The maximum operating pressure of the tube is 376 atm with preheating capability up to 500 K. The shock tube is equipped with a hydraulically operated diaphragm ram section and a custom-designed contour valve for quick vacuuming. To damp out vibrations caused by high pressure experiments, the test section is clamped into a 2-ton concrete dead mass anchored to the floor.

The temperature after the reflected shock (T_5) is calculated from normal shock relations using the obtained shock velocity and normally the ideal equation of state (EoS). However, at elevated pressure, the choice of real gas EoS versus ideal gas EoS for the T_5 calculation needs to be examined in detail. Since the pressure after the reflected shock (P_5) is as high as 200 bar, the density prediction using the ideal gas EoS may not represent the actual density after the reflected shock. Davidson *et al.* [9] derived and solved normal shock relations by implementing real gas equations of state: Peng-Robinson, Soave, Redlich-Kwong and Van der Waals for pure argon up to 1000 atm and temperatures between 1000–3000 K. It was found that when using the Peng-Robinson EoS, there was a 83 K/1000 atm difference when compared to an ideal gas. A similar approach is used in this study and showed a minor deviation of ±4 K in T_5 from ideal gas calculations.

3 Pressure and emission measurements

When diatomic or polyatomic gases are used as diluents, the wall viscous effects (e.g. the thickness of the boundary layer) becomes significantly more noticeable. As a result, the normal portion of the shock wave in the boundary layer turns into a λ-shaped shock near these regions [6], a phenomenon referred to as shock bifurcation. A recent study from Hargis and Petersen [14] showed the significance of the boundary layer effect for gas mixtures with CO_2, Ar and N_2 dilution. The study reported that the thickness of boundary layer is approximately 30 mm in a N_2/CO_2 mixture at 1400 K and 1.83 bar after 600 µs. Therefore, in similar shock tube experiments, the sidewall pressure trace could be contaminated. Another deleterious consequence of the reflected shock-boundary layer interaction is an observed pressure rise after the passage of the reflected shock (i.e. dP_5/dt). In the current work, dP_5/dt derived from sidewall pressure measurements is between 15–18%/ms as demonstrated in Fig. 1a. Correspondingly, the value from endwall traces is between 3–5%/ms for a 5:10:85 mixture of $CH_4/O_2/CO_2$. During the analysis process, the obtained pressure rise over time is simulated in CHMEKIN-PRO [15] for an unbiased comparison between experimental and numerical results. The pressure rise over time (dP_5/dt) were modeled in CHMEKIN-PRO [15] by applying a time-dependent pressure fit using linear regression of the endwall pressure trace.

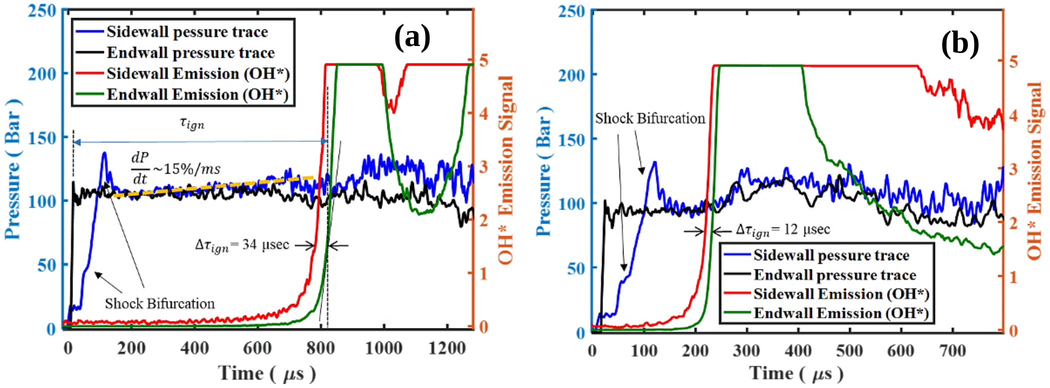

Figure 1. An example of simultaneous sidewall and endwall pressures and OH* emission traces for $CH_4/O_2/CO_2$=5:10:85 at 100 bar and temperature: a) 1274 K and b) 1433 K

To determine the occurrence of autoignition, OH* chemiluminescence is recorded from both sidewall and endwall throughout all experiments. Having fuel concentrations ≥ 2% in the current study, the ignition delay time (τ_{ign}) is defined as the time difference between the arrival of the reflected shock at the endwall and the maximum slope of endwall OH*, as demonstrated in Fig. 1a.

4 Results and discussion

The IDTs for $CH_4/O_2/CO_2$ mixtures at stoichiometric and a fuel-rich conditions (Φ=2) measured at 100 bar and temperature between 1274–1433 K are shown in Fig. 2. The predicted IDTs from different kinetic models are compared with experiments. The simulation results herein are obtained by solving a zero-dimensional reactor with constant internal energy and volume using CHMEKIN-PRO [15]. While USC Mech II [19], Aramco 2.0 [8, 20-25], HP-Mech [26] and FFCM-1 [27] are able to predict IDTs within the uncertainty of the experimental data, GRI 3.0 [7] underpredicts the autoignition delay by a factor of 3.

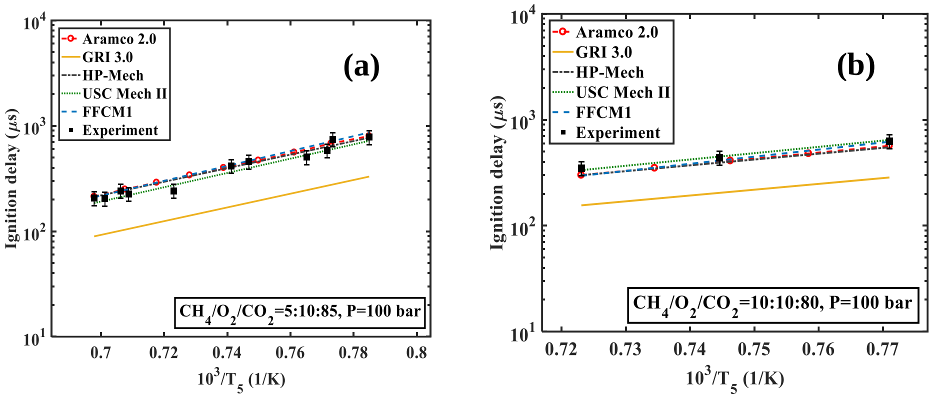

Figure 2. Ignition delay time of $CH_4/O_2/CO_2$ at 100 bar for (a): stoichiometric (Φ =1), T=1274–1433 K (b): rich (Φ =2) mixtures, T=1297–1383 K

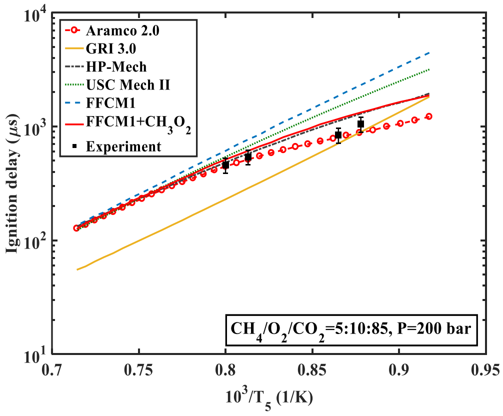

Figure 3. Ignition delay time measurements of stoichiometric $CH_4/O_2/CO_2$ mixtures at 200 bar, T=1139–1250 K

Figure 3 summarizes the results obtained from 200 bar experiments for a 5:10:85 mixture of $CH_4/O_2/CO_2$. At temperatures less than 1250 K, the deviation in IDT predicted by different kinetic models grows while at higher temperature ranges, all kinetic models except for GRI 3.0 [7] show a converging trend. As shown in Fig. 3, the experimental data show very good agreement to IDT predictions from Aramco 2.0 [8, 20-25] for a temperature range of 1139 to 1250 K. HP-Mech [26] also gives a reasonable prediction to the experimental data. FFCM-1 [27], on the other hand, overpredicts the ignition delay at these conditions by approximately a factor of 2.5. GRI 3.0 [7] still fails to predict the ignition trend at 200 bar, having a maximum deviation of approximately 3 times faster ignition delay.

To better understand the behavior of different kinetic models, a reaction pathway flux analysis is conducted. This analysis produces the ratio of carbon flux through different reaction pathways using a Global Pathway Selection (GPS) method [28] in CANTERA [29]. The results for $CH_4/O_2/CO_2$ (5:10:85) at 1200 K and 200 bar is shown in Fig. 4.

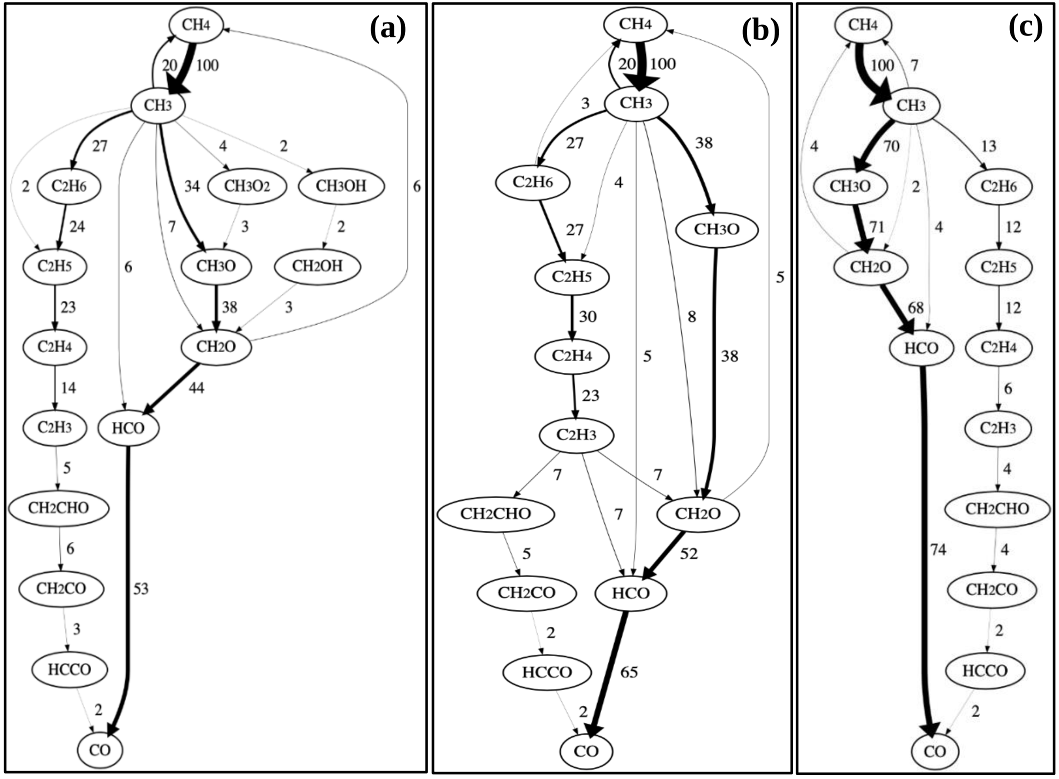

Figure 4. Reaction path flux results for $CH_4/O_2/CO_2$=5:10:85 at 1200 K and 200 bar using (a) Aramco 2.0 (b) FFCM-1 and (c) GRI 3.0

Numbers shown in Fig. 4 represent the percentage of carbon flux (normalized by the total carbon flux of the fuel, CH_4 in this study) through various pathways. After the initiation reaction of CH_4 to form CH_3 (methyl radical), there exist two major reaction pathways of CH_3. One is CH_3 oxidation which is through:

$$CH_3 \rightarrow CH_3O \rightarrow CH_2O \rightarrow HCO \rightarrow CO \tag{1}$$

The second reaction pathway of CH_3 is recombination to form ethane (C_2H_6). Tracking this pathway to formation of CO, pathway (2) for Aramco 2.0 [8, 20-25], pathways (2-4) for FFCM-1 [27] and pathway (2) for GRI 3.0 [7] are observed as following:

$$CH_3 \rightarrow C_2H_6 \rightarrow C_2H_5 \rightarrow C_2H_4 \rightarrow C_2H_3 \rightarrow CH_2CHO \rightarrow CH_2CO \rightarrow HCCO \rightarrow CO \tag{2}$$

$$CH_3 \rightarrow C_2H_6 \rightarrow C_2H_5 \rightarrow C_2H_4 \rightarrow C_2H_3 \rightarrow HCO \rightarrow CO \tag{3}$$

$$CH_3 \rightarrow C_2H_6 \rightarrow C_2H_5 \rightarrow C_2H_4 \rightarrow C_2H_3 \rightarrow CH_2O \rightarrow HCO \rightarrow CO \tag{4}$$

The flux ratio between CH_3 oxidation and recombination pathways (i.e. $CH_3 \rightarrow CH_3O$ and $CH_3 \rightarrow C_2H_6$) for Aramco 2.0 [8, 20-25], FFCM-1 [27] and GRI 3.0 [7] are 1.3, 1.4 and 5.4, respectively. The significantly larger CH_3 oxidation flux ratio explains why GRI 3.0 [7] predicts a much faster autoignition than other two kinetics models.

It can also be seen that two new CH_3 reaction pathways are predicted by Aramco 2.0 [8, 20-25]: formation of CH_3O_2 and CH_3OH which could accelerate autoignition. The experimental data for $CH_4/O_2/CO_2$ mixtures at 200 bar shows a unique trend that is only captured by Aramco 2.0 [8, 20-25]. As observed from Fig. 3, this kinetic model shows a different trend for low and high temperatures. The ignition behavior predicted by Aramco 2.0 [8, 20-25] at 200 bar for the $CH_4/O_2/CO_2$ mixture suggests a strong temperature dependency especially at lower temperatures. A distinct difference is observed in reactions that promote ignition at the two different temperatures. One major difference is the reactions of CH_3O_2 with CH_2O and CH_4, which accelerate oxidation, and therefore promote ignition at 1100 K. At 1400 K, the reaction of CH_3O_2 with CH_3 to form CH_3O becomes relevant for autoignition and the importance of this reaction increases with pressure. Interestingly, the sensitivity analysis performed by Shao *et al.* [10] using FFCM-1 [27] also showed the importance of CH_3O_2 to ignition, while this species is not actually included in FFCM-1 [27]. It can be concluded that the CH_3O_2/CH_3OH kinetics accounts for the unique ignition behavior predicted by Aramco 2.0 [8, 20-25] at low temperature, 200 bar conditions. To further verify the effect of CH_3O_2 in predicting ignition delays at various temperatures, simulations were performed using an improved version of FFCM-1 with the addition of CH_3O_2 kinetics [30]. The results are also presented in Fig. 3. It can be seen that the improved version of FFCM-1 with CH_3O_2/CH_3OH addition matches the experiments well. At high pressure and lower temperature conditions, CH_3 recombines with O_2 to form CH_3O_2, which then oxidizes CH_4 and CH_3 and accelerates ignition.

References

[1] Zhukov VP, Sechenov VA, Starikovskii AY, Spontaneous ignition of methane-air mixtures in a wide range of pressures, Combust. Explos. Shock waves 39 (5) (2003) 487-495.

[2] Petersen EL, Davidson DF, Hanson RK. Ignition Delay Times of Ram Accelerator CH/O/Diluent Mixtures. Journal of Propulsion and Power. 1999;15:82-91.

[3] Vasu SS, Davidson DF, Hanson RK. Shock Tube Study of Syngas Ignition in Rich CO2Mixtures and Determination of the Rate of H + O2+ CO2→ HO2+ CO2. Energy & Fuels. 2011;25:990-7.

[4] Pryor O, Barak S, Koroglu B, Ninnemann E, Vasu SS. Measurements and interpretation of shock tube ignition delay times in highly CO 2 diluted mixtures using multiple diagnostics. Combustion and Flame. 2017;180:63-76.

[5] Koroglu B, Pryor OM, Lopez J, Nash L, Vasu SS. Shock tube ignition delay times and methane time-histories measurements during excess CO 2 diluted oxy-methane combustion. Combustion and Flame. 2016;164:152-63.

[6] Hargis JW, Petersen EL. Methane Ignition in a Shock Tube with High Levels of CO2Dilution: Consideration of the Reflected-Shock Bifurcation. Energy & Fuels. 2015;29:7712-26.

[7] Gregory P. Smith DMG, Michael Frenklach, Nigel W. Moriarty, Boris Eiteneer, Mikhail Goldenberg, C. Thomas Bowman, Ronald K. Hanson, Soonho Song, William C. Gardiner, Jr., Vitali V. Lissianski, and Zhiwei Qin, GRI-Mech 3.0. 1999, Available from: http://www.me.berkeley.edu/gri_mech/.

[8] Zhou C-W, Li Y, O'Connor E, Somers KP, Thion S, Keesee C, et al. A comprehensive experimental and modeling study of isobutene oxidation. Combustion and Flame. 2016;167:353-79.

[9] Davidson DF, Hanson RK. Real Gas Corrections in Shock Tube Studies at High Pressures. Israel J. Chem. 36 (1996) 321-326.

[10] Shao J, Choudhary R, Davidson DF, Hanson RK, Barak S, Vasu S. Ignition delay times of methane and hydrogen highly diluted in carbon dioxide at high pressures up to 300 atm. Proceedings of the Combustion Institute. 2018.

[11] Lemmon EW, Bell, I.H., Huber, M.L., McLinden, M.O. NIST Standard Reference Database 23: Reference Fluid Thermodynamic and Transport Properties-REFPROP. Gaithersburg,: National Institute of Standards and Technology, Standard Reference Data Program,; 2018.
[12] Petersen EL, Hanson RK. Measurement of Reflected-shock Bifurcation Over a Wide Range of Gas Composition and Pressure. Shock Waves. 2006;15:333-40.
[13] Petersen EL, Hanson RK. Nonideal effects behind reflected shock waves in a high-pressure shock tube, Shock Waves 10 (2000) 405-420.
[14] Hargis JW, Petersen EL. Shock-Tube Boundary-Layer Effects on Reflected-Shock Conditions with and Without CO2. AIAA Journal. 2017;55:902-12.
[15] Benson SW, Axworthy Jr AE. Mechanism of the gas phase, thermal decomposition of ozone. The Journal of Chemical Physics. 1957;26:1718-26.
[16] Hong Z, Pang GA, Vasu SS, Davidson DF, Hanson RK. The use of driver inserts to reduce non-ideal pressure variations behind reflected shock waves. Shock Waves. 2009;19:113-23.
[17] Grogan KP, Ihme M. Weak and strong ignition of hydrogen/oxygen mixtures in shock-tube systems. Proceedings of the Combustion Institute. 2015;35:2181-9.
[18] Yamashita H, Kasahara J, Sugiyama Y, Matsuo A. Visualization study of ignition modes behind bifurcated-reflected shock waves. Combustion and Flame. 2012;159:2954-66.
[19] Wang H, You X, Joshi AV, Davis SG, Laskin A, Egolfopoulos F, Law CK. High-Temperature Combustion Reaction Model of H2/CO/C1-C4 Compounds. 2007, Available from: http://ignis.usc.edu/Mechanisms/USC-Mech%20II/USC_Mech%20II.htm
[20] Li Y, Zhou C-W, Somers KP, Zhang K, Curran HJ. The oxidation of 2-butene: A high pressure ignition delay, kinetic modeling study and reactivity comparison with isobutene and 1-butene. Proceedings of the Combustion Institute. 2017;36:403-11.
[21] Burke U, Metcalfe WK, Burke SM, Heufer KA, Dagaut P, Curran HJ. A detailed chemical kinetic modeling, ignition delay time and jet-stirred reactor study of methanol oxidation. Combustion and Flame. 2016;165:125-36.
[22] Burke SM, Burke U, Mc Donagh R, Mathieu O, Osorio I, Keesee C, et al. An experimental and modeling study of propene oxidation. Part 2: Ignition delay time and flame speed measurements. Combustion and Flame. 2015;162:296-314.
[23] Burke SM, Metcalfe W, Herbinet O, Battin-Leclerc F, Haas FM, Santner J, et al. An experimental and modeling study of propene oxidation. Part 1: Speciation measurements in jet-stirred and flow reactors. Combustion and Flame. 2014;161:2765-84.
[24] Metcalfe WK, Burke SM, Ahmed SS, Curran HJ, A hierarchical and comparative kinetic modeling study of C1−C2 hydrocarbon and oxygenated fuels, Int. J. Chem. Kinet. 45 (10) (2013) 638-675
[25] Kéromnès A, Metcalfe WK, Heufer KA, Donohoe N, Das AK, Sung C-J, et al. An experimental and detailed chemical kinetic modeling study of hydrogen and syngas mixture oxidation at elevated pressures. Combustion and Flame. 2013;160:995-1011.
[26] Yang X, Santer J, Zhao H, Ju Y. A high pressure mechanism for H2, CO, CH2O, CH4, CH3OH, C2H2, C2H4, C2H6 with EGR Effects (CO2 and H2O) and HCO prompt reactions 2017.
[27] G.P. Smith YT, and H. Wang. Foundational Fuel Chemistry Model Version 1.0 (FFCM-1). 2016.
[28] Gao X, Yang S, Sun W. A global pathway selection algorithm for the reduction of detailed chemical kinetic mechanisms. Combustion and Flame. 2016;167:238-47.
[29] Goodwin DG, Moffat HK, Speth RL. Cantera: An object- oriented software toolkit for chemical kinetics, thermodynamics, and transport processes. 2.3.0. ed2017.
[30] Wang H. Private Communication Oct. 2018.